Zdravko PRAUNSEIS

University of Maribor, Faculty of Energy Technology, Krsko, Slovenia

doi:10.15199/48.2017.06.11

Determination of the titanium corrosion resistance by nitrogen-ion implantation for applications in electrical engineering

Abstract. *Titanium and alloys are often used in modern electrical engineering. The aim of investigation was to optimize the conditions of nitrogen-ion implantation for commercially pure (CP) titanium and to correlate the implantation parameters with the corrosion resistance. Argon- and oxygen-ion implantations were carried out to compare the corrosion resistance with nitrogen-ion implantation and to understand whether the increased corrosion associated with the nitrogen-ion implantation is a chemical effect produced by the nitrogen or a microstructure change produced by the ion implantation. A surface analysis using Grazing-Incidence X-ray Diffraction (GIXD) was carried out to further understand the role of nitrogen in the corrosion resistance of titanium in the simulated acid fluid. The results of the present investigation indicated that nitrogen-ion implantation can be used as a viable method for improving the corrosion resistance of titanium.*

Streszczenie. *Tytan I jego stopy są często wykorzystywane w nowoczesnej elektrotechnice. Celem tej pracy jest optymalizacja warunków implantacji jonów azotu na komercyjnie czystym tytanie oraz skorelowanie parametrów implantacji z odpornością na korozję. Przeprowadzono implantacje jonów argonu I tlenu w celu porównania odporności korozyjnej z przypadkiem implantacji jonów azotu i uzyskania zrozumienia czy zwiększenie korozji z implanowanymi jonami azotu wynika z efektu chemicznego azotu czy też ze zmiany mikrostruktury spowodowanej implantacją jonów azotu. Analiza powierzchniowa przeprowadzona metodą GIXD (Grazing-Incidence X-ray Diffraction) pozwoliłą wyjaśnić wpływ azotu w na odporność korozyjną tytanu w symulowanym płynie kwasowym. Wyniki przedstawionych badań pokazują, że implantacja jonów azotu jest użyteczną metodą poprawy odporności korozyjnej tytanu. (**Określanie odporności korozji tytanu poprzez implantacje jonów azotowych w zastosowaniach elektrotechnicznych**).*

Keywords: titanium, corrosion, ion implantation, diffraction
Słowa kluczowe: tytan, korozja, impantacja jonów, dyfrakcja

Introduction

The inherent mechanical properties of metallic materials have made them the material of choice for applications in modern electrical engineering, for instance usage for pace-maker casing, protection of electronic circuits and also bimetallic current brining tires [1], and composition elements of individual protection means [2], which operated in the acid environment [3,11,18]. Three alloys – stainless steels, cobalt-chromium alloys and titanium and its alloys – are also the materials used for this type of application. The favorable local-tissue response and the excellent corrosion resistance of titanium and its alloys have promoted their widespread use at the expense of the other two types of metallic materials.

Owing to its enhanced fatigue strength the titanium alloy Ti6Al4V was considered as an interesting alternative to the previously used stainless-steel and cobalt-chromium alloys [8]. However, over the long term the presence of vanadium in this alloy may cause problems, even though the vanadium present in the Ti6Al4V alloy is very stable and the release of vanadium ions under normal conditions is always lower than the toxic level.

The toxicity of vanadium is well known, and it can be aggravated when an implant is fractured and the material subsequently undergoes fretting [4]. This phenomenon may cause local irritation of the tissues surrounding the material. In order to avoid the potential risks several solutions have been proposed. One solution is to continue to use CP titanium as an alternative to this alloy. However, titanium is not inert when it is incorporated into the acid fluid. Titanium releases metallic ions, which subsequently form corrosion products in the acid fluids [5,6]. This phenomenon is more significant in the case of titanium than with stainless steels and cobalt-chromium alloys [7].

Considerable attention had been paid in the recent past to the surface treatment of these materials in order to reduce the problems. For example, ion implantation has been used to improve the mechanical behaviour of these materials [8]. However, less attention has been paid to evaluating the rate of ion release and the corrosion resistance of the modified surfaces.

Nitrogen-ion implantation of the Ti6AV alloy reduced the passive current density in a bio-brine solution. Nitrogen-ion implantation with the same alloy at different doses also influenced the corrosion resistance in the acid fluid [9,10].

In the present research commercially pure (CP) titanium was surface modified with nitrogen-, argon- and oxygen-ion implantations in order to investigate the material's corrosion resistance in a simulated acid fluid. Five doses were chosen for the ions, ranging from $5 \cdot 10^{15}$ cm^{-2} to $2{,}5 \cdot 10^{17}$ cm^{-2}. In-vitro open-cyclic potential (OCP)-time measurements and cyclic polarization studies were carried out to evaluate the corrosion resistance of the modified surface in comparison to an unmodified surface. Specimens implanted at $4 \cdot 10^{16}$ cm^{-2} and $7 \cdot 10^{16}$ cm^{-2} showed the optimum corrosion resistance, higher doses showed a detrimental effect on the corrosion resistance. Argon- and oxygen-ion implantation at these doses did not show any improved corrosion resistance, indicating the beneficial role of nitrogen on the corrosion resistance of titanium in the acid fluid environment. Grazing-incidence X-ray diffraction (GIXD) was employed on the implanted specimens to determine the phases formed with the increasing doses. X-ray photoelectron spectroscopy (XPS) studies on the passive film of the implanted samples and on the unimplanted samples were analyzed in order to understand the role of nitrogen in improving the corrosion resistance. The nature of the surface and the reason for the variation and the improvement in the corrosion resistance are discussed in detail.

Methods and Materials

Commercially pure titanium samples of 8,5 mm diameter were ground with 1000-grit SiC paper and polished with 6 μm and 1 μm diamond pastes. The polished samples were then ultrasonically cleaned with acetone and rinsed with deionized water.

Ion implantation

Nitrogen-, oxygen- and argon-ion implantations were carried out using a 150 kV accelerator at energies of (70, 80 and 140) keV, respectively.

The reason for choosing the different energies was to obtain similar concentration profiles for the implanted ions. Modeling software called TRIM® was used to obtain the concentration profile for each ion as shown in Fig. 1.

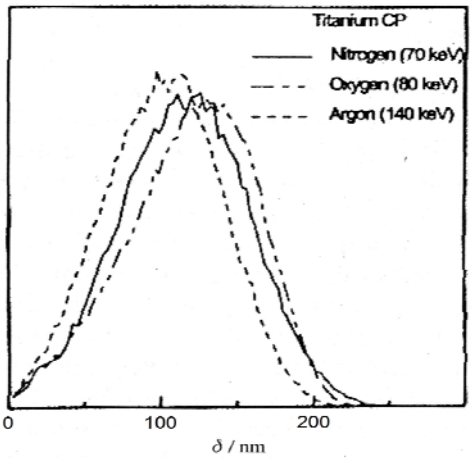

Fig.1. Calculated depth profile δ of N^+-, Ar^+- and O^+- implanted CP titanium

For the nitrogen-ion implantation five different doses were chosen in the range from $5 \cdot 10^{15}$ cm^{-2} to $2{,}5 \cdot 10^{17}$ cm^{-2}.

For the oxygen-and argon-ion implantation three doses were chosen from this range. A summary of the energy and the doses for each ion is given in Table 1.

Table 1. Summary of nitrogen-, argon- and oxygen-ion implantation for different doses

Ion	Nitrogen (70 keV) (cm^{-2})	Argon (140 keV) (cm^{-2})	Oxygen (80 keV) (cm^{-2})
Material-Titanium	$5 \cdot 10^{15}$, $1 \cdot 10^{16}$, $4 \cdot 10^{16}$, $7 \cdot 10^{16}$, $1 \cdot 10^{17}$, $2{,}5 \cdot 10^{17}$	$5 \cdot 10^{15}$, $7 \cdot 10^{16}$, $2{,}5 \cdot 10^{17}$	$5 \cdot 10^{15}$, $7 \cdot 10^{16}$, $2{,}5 \cdot 10^{17}$

Corrosion measurements

Fluid (9,0 g/l NaCl, 0,43 g/l KCl, 0,24 g/l $CaCl_2$ and 0,2 g/l $NaHCO_3$) was used as the electrolyte and maintained at pH 7,4 and 37,4±1 °C to simulate acid fluid conditions in the human body, where the material will operated.

Two electrochemical techniques were used to evaluate the corrosion resistance of the implanted surface in comparison with the untreated surface. In the OCP-time measurements the specimen's potential was monitored as a function of time, starting from the sample's immersion into the electrolyte.

A saturated calomel electrode was used as the reference electrode. For the cyclic polarization test platinum foil was used as the counter electrode.

A scan rate of 1 mV/s was applied to the specimens starting from –750 mV to +2000 mV and then reversed in order to obtain the cyclic polarization curve.

Grazing-incidence X-ray diffraction studies were carried out on the nitrogen-ion-implanted specimens with different doses to understand the phase changes and compound formation after the implantation process. An incidence angel of 1° was used to allow a maximum penetration depth of 0,3 μm for the X-rays into the Ti substrate.

Results and Discussion

Nitrogen-ion implantation

Electrochemical studies

The OCP of the specimens measured as a function of time for nitrogen-ion-implanted samples and the unimplanted samples are presented in Fig. 2.

The OCP of the unimplanted specimens was at the noble potential to begin with; however, after 60 minutes it was shifted to the active potential (+50 mV to –83 mV).

At a very low implantation dose ($5 \cdot 10^{15}$ cm^{-2}) the OCP was initially observed to be at an active potential compared to the unimplanted specimen; however, the OCP moved to a nobler potential with time, when compared to the unimplanted specimen.

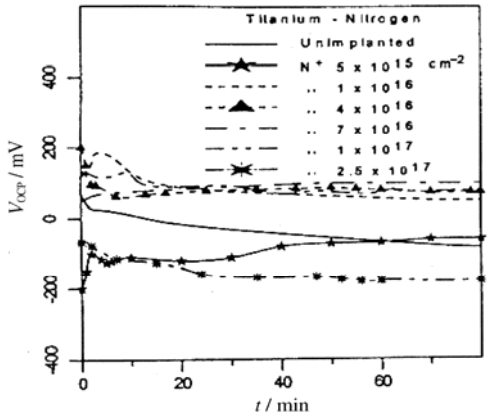

Fig.2. OCP-time measurements of nitrogen-ion-implanted titanium

The OCP was found to shift towards a nobler potential after increasing the doses up to $7 \cdot 10^{16}$ cm^{-2}, and beyond this the OCP started to decrease. The OCP fell drastically to a more negative potential than that of the unimplanted specimen when implanted with a high dose of nitrogen ($2{,}5 \cdot 10^{17}$ cm^{-2}). The moderate doses of $1 \cdot 10^{16}$ cm^{-2} to $1 \cdot 10^{17}$ cm^{-2} not only showed the nobler potential but also a rapid attainment of the steady state was observed.

The enhancement of the potential and the attainment of a stable potential in a short time were attributed to the protective surface layers formed during the implantation. Al-Mayouf et al [12] reported a similar shift of the OCP in the noble direction for implanted specimens and attributed it to the thickening of the native oxide layer formed during the implantation. The shift of the OCP towards the active direction for the nitrogen-ion-implanted specimens at doses above $1 \cdot 10^{17}$ cm^{-2} can be attributed to the sputtering of the oxide layer formed during implantation.

The nitrogen addition may not have a significant role in the OCP of the implanted specimen. Titanium is a passive metal and it undergoes spontaneous passivity when it is placed in an aqueous solution. The change in the OCP would mainly arise from either a thickening of the air-formed passive film or a change in the surface roughness with doses, and/or a combination of both effects.

Figs 3 and 4 are the cyclic polarization curves for the specimens with varying doses of nitrogen-ion implantation.

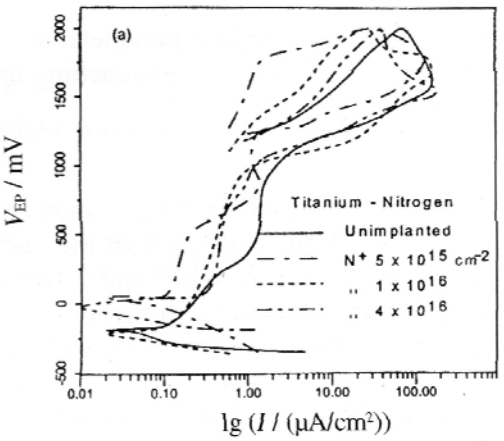

Fig.3. Potentiodynamic cyclic polarization curves for nitrogen-ion-implanted CP titanium in comparison with an unimplanted specimen

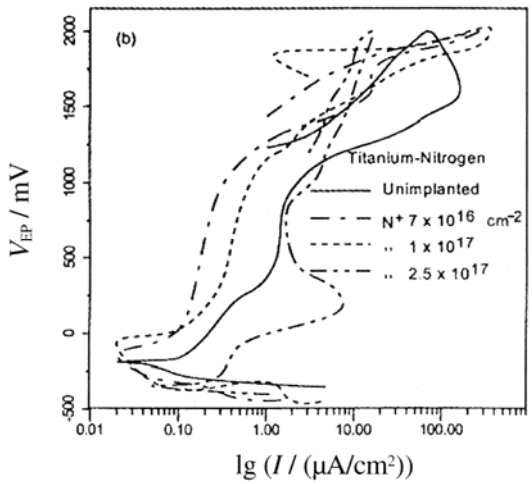

Fig.4. Potentiodynamic cyclic polarization curves for nitrogen-ion-implanted CP titanium in comparison with an unimplanted specimen

Table 2 gives the details of the OCP and the passive current density for all the tested conditions.

Table 2. Corrosion parameters of nitrogen-, argon- and oxygen-ion-implanted CP titanium specimens

Specimens	Open Circuit Potential, V_{OPC} /mV (After 80 minutes)			Passive Current Density, i_{pass} /(μA/cm^2) at 500 mV		
	N^+	Ar^+	O^+	N^+	Ar^+	O^+
Unimplanted	-83	-83	-83	1,2	1,2	1,2
$5\cdot10^{15}$	-46	-23	+19	0,25	0,4	0,34
$1\cdot10^{16}$	+35	-	-	0,33	-	-
$4\cdot10^{16}$	+75	-	-	0,44	-	-
$7\cdot10^{16}$	+110	-129	-39	0,14	0,8	0,52
$1\cdot10^{17}$	+75	-	-	0,31	-	-
$2{,}5\cdot10^{17}$	-150	-145	-41	2,0	0,9	0,8

The implantation at lower doses ($5\cdot10^{15}$ cm^{-2} and $1\cdot10^{16}$ cm^{-2}) showed a lower passive current density and the trend continued up to the specimen implanted at $7\cdot10^{16}$ cm^{-2}.

The specimen implanted at $7\cdot10^{16}$ cm^{-2} showed a minimum passive current density, and beyond this the passive current density started to increase.

The dose of $2{,}5\cdot10^{12}$ cm^{-2} showed a higher passive current density along with an anodic peak at 0–400 mV in the cyclic polarization curve.

The increased passive current density at these doses indicated that the modified surface is prone to corrosion in the simulated body-fluid conditions.

The raid increase in the current density at around 1,2 V for the unimplanted and all the implanted conditions, except the dose of $2{,}5\cdot10^{17}$ cm^{-2}, arises from the oxygen evolution [13].

The samples implanted at $2{,}5\cdot10^{17}$ cm^{-2} did not show a large increase in their current density in this region, indicating the absence of oxygen evolution. The electrical conductivity of the passive film of Ti in the acidic environment is low, and the increase in the anodic potentials leads to a high electrical field across the passive layer.

Under these circumstances ion transport occurs and film growth continues to a thickness of hundreds of nanometers [14].

Though the titanium becomes anodized in the acidic pH, it will not happen in the higher pHs. This was confirmed in the present investigation. The reduction in the oxygen evolution for the specimen implanted at $2{,}5\cdot10^{17}$ cm^{-2} could be attributed to the low electrical conductivity and the growth of the passive film.

GIXD studies

GIXD studies were carried out for the sample that was nitrogen-ion implanted $7\cdot10^{16}$ cm^{-2} and $2{,}5\cdot10^{17}$ cm^{-2} in a comparison with an unimplanted specimen in order to explain the dependence of corrosion resistance on nitrogen fluencies.

The diffraction pattern of the specimens is shown in Fig. 5. The diffraction patterns were scanned in the 2Θ range of 30-55°.

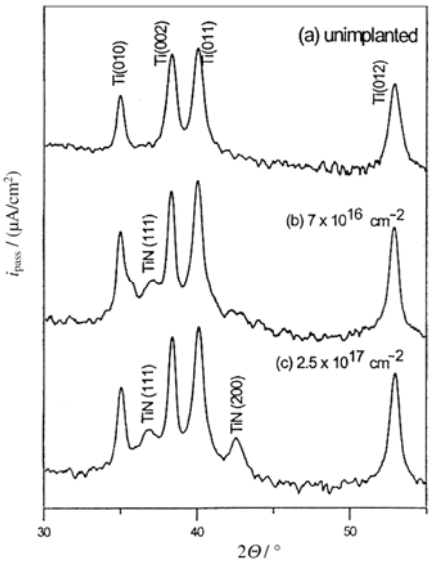

Fig.5. GIXD studies of unimplanted and nitrogen-ion-implanted specimens

The unimplanted specimen showed four peaks, which correspond to the Ti (hcp) peaks.

The specimen implanted with a dose of $7\cdot10^{16}$ cm^{-2} showed a similar pattern to that of unimplanted specimen, but with a small peak at a 2Θ value of 36,85° corresponds to TiN (111). On the other hand, the specimen implanted with a dose of $2{,}5\cdot10^{17}$ cm^{-2} showed two additional peaks, which were indexed to TiN (111) and TiN (200).

It was reported that [15] nitrides start to appear at a dose of $5\cdot10^{16}$ cm^{-2} (50 keV), the size and the number of the precipitates increasing with increase in the dose. Generally, a nitrogen addition will transform the hcp-Ti to bcc-Ti_2N and finally to fcc-Ti_2N and fcc-TiN phases [16]. Also, the lattice parameter may give a rough idea of composition, though care must be taken to account for other possible variations, particularly internal stress. For the atomic ratio of N/Ti=1 the lattice parameter will be 4,2417 nm and the lattice parameter value decreases with decrease in the N/Ti ratio [17].

In the present case, the TiN (111) peak showed a lattice parameter value of 4,2378 nm, which represents the N/Ti ≈ 0,8, from the diagram presented in reference [17]. This indicated the initial stages of nitride formation in the sample implanted at a dose of $7\cdot10^{16}$ cm^{-2}. At still higher doses ($2{,}5\cdot10^{17}$ cm^{-2}), TiN(200) peak showed the lattice parameter of 4,2411 nm with respect to N/Ti ratio approaching unity.

The role of nitrogen in the corrosion resistance of titanium

The nitrogen-ion-implanted titanium showed marked changes in its corrosion resistance with the variation in the doses. The doses between $4\cdot10^{16}$ to $7\cdot10^{16}$ cm^{-2} were found to be the optimum, with higher doses having a detrimental

effect. The improvement in the passivity in the simulated acid fluid condition may be due to the following reason: The availability of a large amount of nitrogen at the surface will make the surface inactive by resisting the interaction with the reactive O_2^- and Cl^- with titanium.

Nitrogen present in the implanted layers in the solid solution forms oxynitrides during the cyclic polarization and enhances the corrosion resistance.

Our XPS results showed the formation of oxynitrides in the passive film of the implanted specimen. At higher doses, the titanium forms its nitrides, which introduces the metallurgical inhomogenities to the surface. These nitrides tend to detach from the metallic matrix and form a galvanic couple with the metal matrix. As a result, the nitride precipitate will remain as a cathodic and the other metal surface will undergo the active dissolution, and hence an increased current density was observed.

Argon - ion implantation

Fig. 6 shows the OCP-time measurement for the argon-ion-implanted titanium specimens.

The implantation carried out at low doses ($5 \cdot 10^{15}$ cm^{-2}) showed a sharp decrease in the OCP at the initial stage and attained a steady state at around –20 mV which is a nobler shift compared to the unimplanted specimen. However, the specimen implanted at $7 \cdot 10^{16}$ cm^{-2} and $2{,}5 \cdot 10^{17}$ cm^{-2} showed a shift in the OCP, which were far more negative than the unimplanted condition.

Though the OCP of the specimen implanted at $7 \cdot 10^{16}$ cm^{-2} was lower than the unimplanted specimen, it achieved the steady state much earlier.

However, the specimen implanted at $2{,}5 \cdot 10^{17}$ cm^{-2} showed the lowest OCP values (-120 mV) with fluctuation, and it could not achieve the steady state during a measurement up to 60 minutes. The shift of the OCP to a more negative potential suggests that argon-ion implantation enhances the activity of the metal surface. The potentiodynamic cyclic polarization behaviour of Ar-ion-implanted titanium specimens are shown in Figure 7. The specimen implanted at $5 \cdot 10^{15}$ cm^{-2} showed a reduction in the passive current density compared to the unimplanted condition.

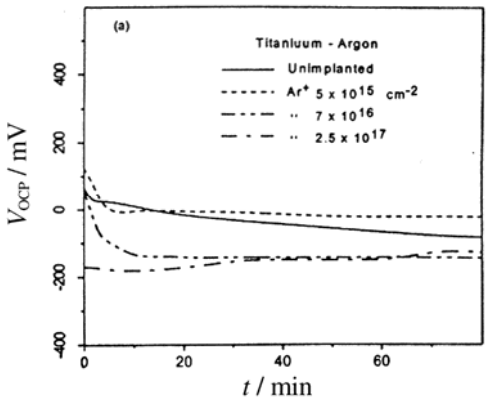

Fig.6. OCP-time measurements

However, compared with nitrogen-ion implantation of the same dose, the reduction is not significant. The doses exhibiting the smallest current density ($7 \cdot 10^{16}$ cm^{-2}) in the nitrogen-ion implantation did not show a significant reduction in their passive current density for argon-ion implantation. At high doses of argon-ion implantation ($2{,}5 \cdot 10^{17}$ cm^{-2}) the current density was still higher, suggesting the dissolution of the metals.

The specimen showed a hump at –300 to –50 mV, which in the cathodic region indicates a high degree of cathodic reaction on the surface that is in the air-formed oxide film.

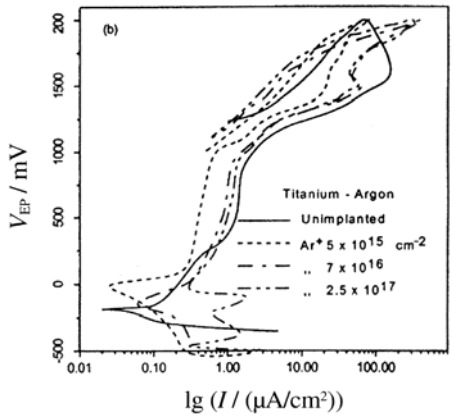

Fig.7. Cyclic polarization curves for argon-ion-implanted titanium

Oxygen-ion implantation

Fig. 8 shows the OCP-time measurements of oxygen-ion-implanted titanium specimens at three different doses compared to the unimplanted specimen. All the implanted specimens showed a shift in the OCP towards a nobler direction and attained a steady state in a short time.

The specimen implanted at $5 \cdot 10^{15}$ cm^{-2} reached a potential of +20 mV in the 80 minutes. The other two doses showed the value of –20 mV.

The noble shift for the all implanted specimen is attributed to the stable surface layers produced by oxygen-ion implantation.

In the case of N- and Ar-ion implantations, the high dose ($2{,}5 \cdot 10^{17}$ cm^{-2}) specimens showed lower OCP values than the unimplanted specimen.

The noble value obtained in the O-ion implantation may be attributed to the formation of oxides during implantation layer, which resist the dissolution.

Cyclic polarization showed a similar trend to OCP time measurements (Figure 9). All the implanted specimens showed a lower passive current density than the unimplanted specimen.

The specimens implanted at $2{,}5 \cdot 10^{17}$ cm^{-2} did not show any hump in the cathodic region and/or in the initial stages of anodic oxidation, indicating that there is dissolution at this region. Like the Ar-ion implantation it also exhibited the peak at +1.2 V, which is responsible for the oxygen evolution.

In summary, Ar- and O-ion implantations showed a marginal improvement for low dose of Ar-ion implantation and the dose ranging from $5 \cdot 10^{15}$ cm^{-2} to $2{,}5 \cdot 10^{17}$ cm^{-2} for the O-ion implantation.

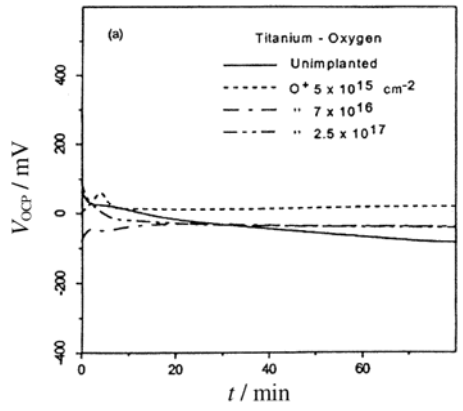

Fig.8. OCP-time measurements

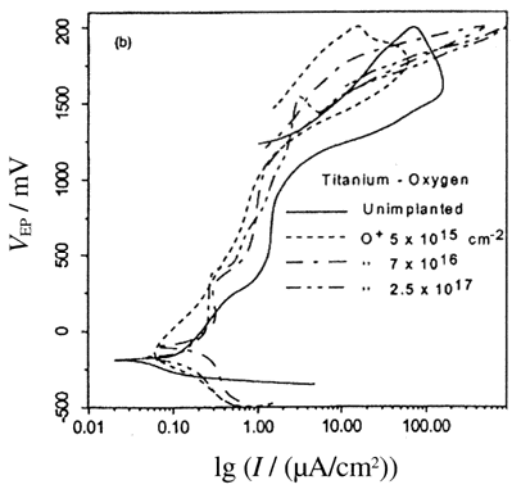

Fig.9. Cyclic polarization curves for oxygen-ion-implanted titanium

However, the improvements observed in these implantations are much lower when compared to N-ion implantation.

The variation in the corrosion parameters of the implanted specimens clearly indicated the improvement in the corrosion resistance as a result of N-ion implantation is purely a chemical effect produced by nitrogen.

Conclusion

Nitrogen-ion implantation on commercially pure (CP) titanium showed an improvement in the electrochemical behaviour of the passive film. The optimum doses between $4 \cdot 10^{16}$ cm^{-2} and $7 \cdot 10^{16}$ cm^{-2} are recommended for electrical engineering applications in the acid environment.

Higher doses showed a detrimental effect due to the formation of nitrides. Argon- and Oxygen-ion implantations did not improve the corrosion resistance significantly compared to the nitrogen-ion implantation.

Acknowledgements

The authors wish to acknowledge the financial support of the Slovenian Foundation of Science and Technology and the Japanese Promotion of Science.

***Author**: assistant prof. dr. Zdravko Praunseis, University of Maribor, Faculty of Energy Technology, Hocevarjev trg 1, 8270 Krsko, Slovenia, E-mail: zdravko.praunseis@um.si;*

REFERENCES

[1] Shapoval, A.A., Mos'pan, D.V. & Dragobetskii, V.V. Ensuring High Performance Characteristics For Explosion-Welded Bimetals // *Metallurgist*, July 2016, Volume 60, Issue 3, pp 313–317. DOI: 10.1007/S11015-016-0292-9

[2] Dragobetskii, V.V., Shapoval, A.A., Zagoryanskii, V.G. Development of Elements of Personal Protective Equipment of New Generation on the Basis of Layered Metal Compositions // *Steel in Translation*, 2015, Vol. 45, Issue 1, © Allerton Press, Inc., pp. 33–37. DOI: 10.3103/S0967091215010064

[3] Pan J., Thierry D., Leygraf C., Electrochemical impedance spectroscopy study of the passive oxide film on titanium for pace-maker application, *Electrochimica Acta,* 41(2014), No. 7, 1143-1153

[4] Shukla AK., Balasubramaniam R., Bhargava S., Properties of passive film formed on CP titanium, Ti-6Al-4V and Ti-13.4Al-29Nb alloys in simulated acid conditions, *Intermetallics*, 13 (2005), No. 6, 631-637

[5] Koike M., Fujii H., In vitro assessment of corrosive properties of titanium as a biomaterial, *Journal of Oral Rehabilitation*, 2 (2001), No. 1, 34-39

[6] American Society for Metals Handbook, Corrosion, *Materials Park*, ASM International, 1993

[7] Boere G., Influence of fluoride on titanium in an acidic environment measured by polarization resistance technique, *Journal of Applied Biomaterials*, 6 (1995), No. 4, 283-288

[8] Schiff N., Grosgogeat B., Lissac M., Dalard F., Influence of fluoride content and pH on the corrosion resistance of titanium and its alloys, *Biomaterials*, 23 (2002), No. 9, 1995-2002

[9] Di Schino A., Kenny JM., Effects of the grain size on the corrosion behavior of refined AISI 304 austenitic stainless steels, *Journal of Materials Science Letters*, 21 (2002), No. 20, 1631-1634

[10] Balakrishnan A., Lee BC., Kim TN., Corrosion behavior of ultra fine grained titanium in simulated acid fluid for implant application, *Trends in Biomaterials and Artificial Organs*, 13 (2008), No. 2, 123-127

[11] Praunseis Z., Sundararajan T.,Toyoda M., Fracture behaviours of fracture toughness testing specimens with metallurgical heterogeneity along crack front, *Steel Research*, 71 (2008), No. 3, 366-373

[12] Al-Mayouf AM., Al-Swayih AA., Corrosion behavior of a new titanium alloy for dental implant applications in fluoride media, *Materials Chemistry and Physics*, 86 (2004), No. 2, 320-329

[13] Fontana MG., Corrosion Engineering, New York, *McGraw-Hill Book*, Company, 1986

[14] Amstutz HC., Campbell P., Kossovsky N., Mechanism and clinical significance of wear debris-inducedosteolysis, *Clinical Orthopedics and Related Research*, 11 (2002), 276-283

[15] Black J., Sherk H., Metallosis associated with a stable titanium-alloy femoral component in total hipreplacement, A case report, *Journal of Bone and Joint Surgery*, 15 (1990), No. 3, 111-129

[16] Sungern J., *Thin Solid Films*, 12 (1995), No. 5, 21-24

[17] Toth L. E., Transition of metal carbides and nitrides, *Academic Press*, New York, 1997

[18] Praunseis Z., Sundararajan T., The influence of soft root on fracture behaviours of high strenght low alloyed steel, *Materials and Manufacturing Processes*,16 (2001), No. 6, 229-244